

Accepted Manuscript

Efficient Delivery of Therapeutic Small Nucleic Acids to Prostate Cancer Cells Using Ketal Nucleoside Lipid Nanoparticles

Delphine Luvino, Salim Khiati, Khalid Oumzil, Palma Rocchi, Michel Camplo, Philippe Barthélémy

PII: S0168-3659(13)00794-3
DOI: doi: [10.1016/j.jconrel.2013.09.006](https://doi.org/10.1016/j.jconrel.2013.09.006)
Reference: COREL 6880

To appear in: *Journal of Controlled Release*

Received date: 24 April 2013
Accepted date: 5 September 2013

Please cite this article as: Delphine Luvino, Salim Khiati, Khalid Oumzil, Palma Rocchi, Michel Camplo, Philippe Barthélémy, Efficient Delivery of Therapeutic Small Nucleic Acids to Prostate Cancer Cells Using Ketal Nucleoside Lipid Nanoparticles, *Journal of Controlled Release* (2013), doi: [10.1016/j.jconrel.2013.09.006](https://doi.org/10.1016/j.jconrel.2013.09.006)

This is a PDF file of an unedited manuscript that has been accepted for publication. As a service to our customers we are providing this early version of the manuscript. The manuscript will undergo copyediting, typesetting, and review of the resulting proof before it is published in its final form. Please note that during the production process errors may be discovered which could affect the content, and all legal disclaimers that apply to the journal pertain.



Efficient Delivery of Therapeutic Small Nucleic Acids to Prostate Cancer Cells Using Ketal Nucleoside Lipid Nanoparticles

*Delphine Luvino,^{‡, #} Salim Khiati,^{‡, #} Khalid Oumzil,^{‡, #} Palma Rocchi,^{‡, *} Michel Camplo,^{‡, *}
and Philippe Barthélémy^{‡, #, *}*

[‡] Univ. Bordeaux, ARNA laboratory, F-33000 Bordeaux, France

[#] INSERM, U869, ARNA laboratory, F-33000 Bordeaux, France

[‡] Aix-Marseille University, CNRS, CINaM UMR 7325, 13288 Marseille cedex 9, France.

[‡] INSERM U1068, CNRS UMR 7258, Institut Paoli-Calmettes, Aix-Marseille Université, 13009 Marseille, France

* corresponding authors: palma.rocchi@inserm.fr, camplo@univmed.fr and philippe.barthelemy@inserm.fr

Keywords: siRNA, antisense, drug delivery, nucleoside lipids, prostate cancer

Abstract: A novel nucleoside lipid derived from dioleoyl ketal was synthesized from uridine in three steps starting from dioleoyl ketone. Electronic microscopy studies show that Ketals Nucleoside Lipids (KNL) self-assemble to form liposome-like structures in aqueous solutions. KNL is able to bind siRNA as demonstrated by electrophoresis experiment and standard ethidium bromide fluorescence displacement assay. Transfection assays of stable hepatic cell lines HupIRF, carrying a luciferase reporter gene demonstrate that KNL is able to transfect siRNA and exhibits protein knockdown more efficiently than its diester analogue (DOTAU) and lipofectamine. Herein, we also report that KNLs are suitable transfecting reagents for the development of novel therapeutic approaches involving either siRNA or antisense oligonucleotide against human prostate cancer PC-3 cells resistant to chemotherapy.

INTRODUCTION

Small interfering RNA (siRNA) are promising therapeutic agents against a large diversity of diseases, including cancer,^{i,ii} and infections^{iii,iv}. The development of efficient and safe siRNA delivery systems remains the main challenge for clinical applications, since these polyanions cannot pass through cellular membranes. Hence, numerous systems^{v,vi,vii,viii} have been developed to improve their stability^{ix,x,xi} and their cellular uptake^{xii,xiii}. Among the non-viral systems developed so far, cationic lipids remains one of the most abundant classes of transfecting reagents used nowadays in laboratories. Recently, a rational approach to design cationic lipids was developed by Semple *et al.* for delivering siRNA.^{xiv} In this study the transfection efficiency of a series of cationic lipids analogues to 1,2-dilinoleyloxy-3-dimethylaminopropane (DLinDMA) was realized *in vivo*. The authors demonstrated that a lipid featuring a ketal linker between the polar head and lipid chains was well tolerated in primates; moreover, this lipid was the best performing transfecting lipid of the series investigated. Likewise, it was recently reported that a pH-sensitive lipid featuring a ketal function facilitated the delivery of liposomal siRNA and gene silencing activity both *in vitro* and *in vivo*.^{xv}

Among cationic transfecting reagents, amphiphiles having a double functionality based on the combination of nucleic acid and lipid characteristics have shown to be efficient transfecting reagent for both plasmid DNA^{xvi} and siRNA^{xvii,xviii} with poor toxicity. In parallel, our groups reported a new family of zwitterionic ketal based nucleolipids (KNLs), which can be used to construct complementary supramolecular systems *via* molecular recognition between individual nucleolipids (NLs) derived from uridine and adenosine.^{xix,xx} These studies showed that the base pair interactions between the nucleolipids polar heads were favoured by the ketal linker, which restricts the ribose cycle in the southern conformation (C2'-endo). Based upon both these results and the transfecting data obtained by Semple *et al.*, we hypothesized that the modification of the chemical structure and conformations of the ribose moiety could have an impact on the siRNA/nucleolipid stability and siRNA delivery. Hence, the chemical structure of the cationic nucleolipid DOTAU (figure 1), which is a key components in transfection formulations, was modified *via* the insertion of a ketal linker at the 2' and 3' positions.

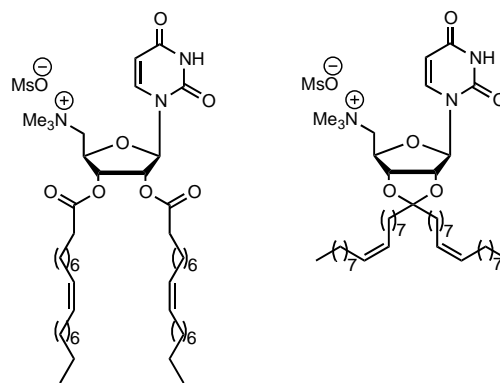


Figure 1. Chemical structure of cationic nucleotide-lipids used in this study (left: DOTAU and its ketal analogue: right).

In this contribution, we report a new non-viral transfecting system belonging to the nucleolipids family. We demonstrate that ketal based nucleolipids, which are non-toxic cationic bioinspired amphiphiles, provide an efficient siRNA carrier. Their ability to transfect siRNA in human hepatic cell lines HupIRF, carrying a luciferase reporter gene, has been examined and compared with lipofectamine. Furthermore, *in vitro* transfection experiments demonstrate that KNLs are suitable molecules for the development of novel therapeutic approaches involving either siRNA or antisense oligonucleotide against human prostate cancer PC-3 cells resistant to chemotherapy.

MATERIALS AND METHODS

Experimental part.

Unless noted otherwise, all starting materials were purchased from Sigma-Aldrich, Acros, or Alfa Aesar and used as received. Some solvents were distilled under argon over appropriate drying agent: tetrahydrofuran and diethylether over sodium/benzophenone, dichloromethane over CaCl_2 . Unless otherwise stated, the other solvents were used as commercially available. All the reactions were conducted under an argon atmosphere unless otherwise stated. All the glassware used was oven-dried.

All compounds were characterized by ^1H NMR, ^{13}C NMR, and mass spectroscopy. ^1H NMR and ^{13}C NMR spectra were recorded at 20 °C on a Bruker spectrometer at 250 MHz (^1H) and 62.5 MHz (^{13}C). Chemical shifts are given in ppm referenced to the solvent residual peak (^1H , CDCl_3 , 7.26 ppm; and ^{13}C , 77 ppm). The ^1H NMR coupling constants (J) are reported in hertz. ESI-MS and elemental analyses were performed at the spectropole of the Aix-Marseille Université, Saint-Jerôme, Marseille, France. Electrospray ionization mass spectra (ESI-MS) were recorded with an API//Plus sciex triple quadripole spectrophotometer in the positive mode. TEM microscopy experiments were performed on a Philipps CM10 (negative staining with ammonium molybdate 1% in water, Cu/Pd carbon coated grids). Analytical thin layer chromatography (TLC) was performed on precoated glass plates with Kieselgel 60F254 neutral with aluminum support plate (0.25 mm layer thickness), SDS.

Compounds were revealed by UV light (254 nm) after spraying with 5% sulfuric acid ethanol solution and heating.

Column chromatography was performed on Merck silica gel 60 (0.063–0.200 mm) or silica gel reverse phase C18.

Ethyl oleate (2)^{xxi} or (Z)-ethyl-9-octadecenoate

Oleic acid (5 g, 18 mmol) and para-toluene sulfonic acid (42 mg, 0.22 mmol) were suspended in EtOH-toluene (1:5; 50 mL) under an argon atmosphere. The reaction mixture was stirred under reflux for 12 hours, using a Dean Stark apparatus.

After removal of the solvent under reduced pressure, the residue was dissolved in diethyl ether (50 mL) and washed with saturated NaHCO₃ (3 x 50 mL). The organic layer was dried over Na₂SO₄ and concentrated in vacuo to give 5.31 g (96%) of **2** as a colourless liquid. The crude product was no further purified.

¹H NMR (250 MHz, CDCl₃): δ = 0.87 (t, *J* = 6.2 Hz, CH₃_{oleyl}, 3 H), 1.27 (m, (CH₂)₁₀ + CH₃_{ethyl}, 23 H), 1.61 (m, CH₂-CH₂C=O, 2 H), 2.00 (m, CH₂-CH=CH-CH₂, 4 H), 2.28 (t, *J* = 7.4 Hz, CH₂-COOEt, 2 H), 4.11 (q, *J* = 7.1 Hz, CH₂_{ethyl}, 2 H), 5.33 (td, *J* = 1.7 Hz, *J* = 5.5 Hz, -CH=CH-, 2 H).

¹³C NMR (62.5 MHz, CDCl₃): δ = 14.1, 22.6, 25.0, 27.1, 27.2, 29.1 (2), 29.2 (2), 29.3, 29.5, 29.6, 29.7, 31.9, 34.4, 60.1, 129.8, 130.0, 173.8.

MS (ESI⁺): *m/z* (%) = 311 (100) [M + H]⁺ HRMS (ESI⁺): *m/z* calcd for C₂₀H₃₉O₂ (M + H⁺): 311.2945; found: 311.2944.

(9Z, 28Z)-19-[(7Z)-7-hexadecenyl]-9,28-heptatriacontadiene-18,20-dione (3)

Ethyl oleate (5 g, 16 mmol) and freshly prepared sodium ethylate (548 mg, 8 mmol) were stirred and warmed under reduced pressure until the reaction was completed (no more boiling ethanol). The reaction was next allowed to reach room temperature and acetic acid (30%, 3 mL) was added. The residue was dissolved in dichloromethane (100 mL) and washed with brine (3 x 50 mL). The organic layer was dried over Na₂SO₄ and concentrated in vacuo to give 4.55 g (49%) of **3** as a yellow oil, which was not further purified.

¹H NMR (250 MHz, CDCl₃): δ = 0.88 (t, *J* = 6.8 Hz, 2CH₃_{oleyl}, 6 H), 1.27 (m, (CH₂)₂₀ + CH₃_{ethyl}, 43 H), 1.61 (m, CH₂-CH₂(C=O), 2 H), 1.83 (m, CH₂-CH(C=O)₂, 2 H), 2.07 (m, CH₂-CH=CH-CH₂, 8 H), 2.48 (t, *J* = 7.7 Hz, CH₂-(C=O)CHCOOEt, 2 H), 3.40 (t, *J* = 7.2 Hz, CH-(C=O)₂, 1 H), 4.16 (q, *J* = 7.3 Hz, CH₂_{ethyl}, 2 H), 5.33 (m, -CH=CH-, 4 H).

¹³C NMR (62.5 MHz, CDCl₃): δ = 14.1 (2), 17.4, 22.9 (2), 24.1, 26.9, 27.2, 27.3 (2), 27.4 (2), 29.0, 29.1 (2), 29.3 (2), 29.4, 29.5 (4), 29.6, 29.7 (2), 29.8 (2), 30.9, 31.9, 40.4, 59.2, 60.1, 129.6, 129.7, 129.9 (2), 170.0, 204.2.

MS (ESI⁺): m/z (%) = 575 (100) [M + H]⁺ HRMS (ESI⁺): m/z calcd for C₃₈H₇₁O₃ (M + H⁺): 575.5398; found: 575.5391.

Oleone (4)

The previously obtained compound **3** (4.9 g, 8.5 mmol) was dissolved in an ethanolic solution of KOH (5 %, 3.5 g in 70 mL of EtOH). The mixture was stirred under reflux for 4 hours and then allowed to warm to room temperature. The volatiles were concentrated under reduced pressure and the mixture was diluted with CH₂Cl₂ (100 mL) and successively washed with brine and aqueous HCl 1N. The organic layer was dried on Na₂SO₄, filtered and concentrated under reduced pressure. The residue was purified by flash column chromatography (n-hexane/EtOAc: 95/5) to give **4** (4.4 g, 95 %) as colourless oil.

¹H NMR (250 MHz, CDCl₃): δ = 0.88 (t, J = 6.3 Hz, 2CH₃_{oleyl}, 6 H), 1.30 (m, (CH₂)₂₁, 42 H), 1.64 (m, CH₂-CH₂(C=O), 2 H), 2.00 (m, CH₂-CH=CH-CH₂, 8 H), 2.34 (t, J = 7.5 Hz, (CH₂)₂-(C=O), 4 H), 5.34 (m, -CH=CH-, 4 H).

¹³C NMR (62.5 MHz, CDCl₃): δ = 14.1 (2), 22.7 (2), 24.7 (2), 26.9 (2), 27.1 (2), 27.2 (2), 27.3 (2), 29.0 (2), 29.1 (2), 29.3 (2), 29.4 (2), 29.5 (2), 29.7 (2), 29.8 (2), 31.9 (2), 33.7 (2), 129.7 (2), 210.3.

MS (ESI⁺): m/z (%) = 520 (100) [M + NH₄⁺]⁺ HRMS (ESI⁺): m/z calcd for C₃₅H₇₀NO (M + NH₄⁺): 520.5452; found: 520.5454.

2', 3'-dioleoyl ketal uridine (5)

Uridine (1.2 g, 4.92 mmol) was dissolved in freshly distilled THF under an argon atmosphere, and oleone **4** (500 mg, 0.99 mmol), CH(OEt)₃ (750 μL, 4.92 mmol) and pTsOH (188 mg, 1 mmol) were added. The mixture was stirred under reflux for 3 days then allowed to warm to room temperature and triethylamine (300 μL) was added. After stirring for 1 hour, the mixture was partitioned between CH₂Cl₂ (300 mL) and saturated aqueous NaHCO₃ solution. The organic layer was washed with brine, dried on Na₂SO₄, filtered and concentrated under reduced pressure. The residue was purified by flash column chromatography (CH₂Cl₂/EtOAc: 80/20) to give **5** (234 mg, 32 %) as colourless oil.

¹H NMR (250 MHz, CDCl₃): δ = 0.87 (t, J = 6.5 Hz, 2CH₃_{oleyl}, 6 H), 1.31 (m, (CH₂)₂₂, 44 H), 1.56-1.76 (m, CH₂-C(O)₂, 4 H), 1.99 (m, CH₂-CH=CH-CH₂, 8 H), 3.77-3.93 (m, H_{5'}, H_{5''}, 2 H), 4.28 (m, H_{4'}, 1 H), 4.95 (m, H_{3'}, 1 H), 5.03 (m, H_{2'}, 1 H), 5.32 (m, -CH=CH-, 4 H), 5.55 (d, J = 2.7 Hz, H_{1'}, 1 H), 5.72 (d, J = 8.1 Hz, H₅, 1 H), 7.35 (d, J = 8.2 Hz, H₆, 1 H).

^{13}C NMR (62.5 MHz, CDCl_3): δ = 14.0 (2), 22.6 (2), 23.5, 24.1, 27.1 (2), 27.3 (2), 29.1 (2), 29.2 (2); 29.3 (2), 29.4 (4), 29.6 (2), 29.7 (2), 31.8 (2), 36.8 (2), 36.9 (2), 58.1, 80.3, 84.0, 87.3, 95.5, 102.3, 118.2, 129.6 (2), 129.8 (2), 142.9, 150.4, 163.8.

MS (ESI⁺): m/z (%) = 729 (100) $[\text{M} + \text{H}^+]^+$ HRMS (ESI⁺): m/z calcd for $\text{C}_{44}\text{H}_{77}\text{N}_2\text{O}_6$ ($\text{M} + \text{H}^+$): 729.5776; found: 729.5778.

2', 3'-dioleylketal-5'-O-mesyuridine (6)

2', 3'-dioleylketal uridine **5** (2.0 g, 2.7 mmol) was dissolved in dry dichloromethane (50 mL) under argon atmosphere and the solution was cooled to 0°C. DMAP (1.35 g, 11 mmol) was added followed by mesyl chloride (850 μL , 11 mmol) dropwise. After the addition, the solution was allowed to warm to room temperature, stirred overnight, and was quenched with methanol. The resulting mixture was stirred for 30 min, diluted with CH_2Cl_2 (100 mL) and successively washed with brine and aqueous NaHCO_3 . The organic layer was dried on Na_2SO_4 , filtered and concentrated under reduced pressure. The residue was purified by flash column chromatography ($\text{CH}_2\text{Cl}_2/\text{EtOAc}$: 80/20) to give **6** (1.63 g, 75 %) as a colourless oil.

^1H NMR (250 MHz, CDCl_3): δ = 0.87 (t, J = 5.1 Hz, 2CH_3 oleyl, 6 H), 1.27 (m, $(\text{CH}_2)_{22}$, 44 H), 1.54-1.71 (m, $\text{CH}_2\text{-C}(\text{O})_2$, 4 H), 2.00 (m, $\text{CH}_2\text{-CH=CH-CH}_2$, 8 H), 3.02 (s, CH_3 mesyl, 3 H), 4.42 (m, H_5' , H_5'' , H_4' , 3 H), 4.86 (m, H_2' , 1 H), 5.06 (m, H_3' , 1 H), 5.33 (m, -CH=CH- , 4 H), 5.56 (m, H_1' , 1 H), 5.75 (d, J = 7.6 Hz, H_5 , 1 H), , 7.24 (d, J = 7.9 Hz, H_6 , 1 H).

^{13}C NMR (62.5 MHz, CDCl_3): δ = 14.4 (2), 23.6 (2), 24.7, 25.1, 27.1 (2), 29.0, 29.3 (2), 29.4 (4), 29.5 (8), 29.6 (2), 29.8 (2), 31.8 (2), 36.8, 37.6, 69.1, 81.2, 84.5, 85.9, 96.6, 102.8, 118.5, 129.7 (4), 143.3, 150.2, 163.6.

MS (ESI⁺): m/z (%) = 824 (100) $[\text{M} + \text{NH}_4^+]^+$ HRMS (ESI⁺): m/z calcd for $\text{C}_{45}\text{H}_{82}\text{N}_3\text{O}_8\text{S}$ ($\text{M} + \text{NH}_4^+$): 824.5817; found: 824.5816.

Mesylate salt of N-[5'-(2',3'-dioleyl)uridine ketal]-N',N',N'-trimethylammonium (7)

Anhydrous trimethylamine (1mL) was transferred to a pressure tube cooled at -50°C via a syringe. Next, anhydrous freshly distilled THF (1 mL) and a solution of **6** (320 mg, 0.4 mmol) in dry THF were added. The tube was sealed and heated in an oil bath at 50°C during 48 h and then cooled to -20°C and opened. The solvents were evaporated under reduced pressure and the residue was purified by reverse phase flash column chromatography ($\text{H}_2\text{O}/\text{MeOH}$: 20/80) to give **7** (254 mg, 74 %) as colourless oil.

^1H NMR (250 MHz, CDCl_3): δ = 0.93 (t, J = 6.2 Hz, 2CH_3 _{oleyl}, 6 H), 1.36 (m, $(\text{CH}_2)_{22}$, 44 H), 1.63-1.83 (m, $\text{CH}_2\text{-C(O)}_2$, 4 H), 2.06 (m, $\text{CH}_2\text{-CH=CH-CH}_2$, 8 H), 2.72 (s, CH_3 _{mesyl}, 3 H), 3.23 (s, $(\text{CH}_3)_3\text{N}$, 9 H), 3.86 (m, H_5' , H_5'' , 2 H), 4.59 (m, H_4' , 1 H), 4.90 (m, H_2' , 1 H), 5.14 (m, H_3' , 1 H), 5.37 (m, -CH=CH- , 4 H), 5.72 (d, J = 8 Hz, H_5 , 1 H), 5.83 (d, J = 1.4 Hz, H_1' , 1 H), 7.71 (d, J = 8.1 Hz, H_6 , 1 H).

^{13}C NMR (62.5 MHz, CDCl_3): δ = 14.6 (2), 23.7 (2), 24.8, 25.2, 28.1 (2), 30.2 (2), 30.3 (2), 30.4 (4), 30.5 (6), 30.6 (2), 30.8 (2), 33.0 (2), 37.3, 38.1, 39.6, 54.7 (3), 69.2, 83.1, 84.6, 84.9, 96.9, 103.3, 119.9, 130.7 (4), 145.4, 151.9, 165.8.

MS (ESI^+): m/z (%) = 770 (100) [M^+] $^+$. HRMS (ESI^+): m/z calcd for $\text{C}_{47}\text{H}_{84}\text{N}_3\text{O}_5^+$ (M^+): 770.6406; found: 770.6405.

Vesicle Preparation. 10 mg of compounds (lipids, KNL etc.) was dissolved in 1 mL of chloroform. 50 μL of this solution were placed in glass tube and the chloroform was evaporated and dried under vacuum for 2 h. 1 mL of DI water was added, and the solution was hydrated overnight at 4°C . Prior to measurement, the resulting solution was sonicated for 20 min and was extruded through a polycarbonate filter (100 nm) 10 times to obtain small unilamellar vesicles at 0.5 mg/mL final concentration.

Electrophoresis Studies:

Agarose gel analysis. Electrophoresis studies were conducted in 2% agarose gels containing ethidium bromide in a 0.5 Tris-Borate-EDTA buffer. Cationic lipoplexes were prepared 10 min before use. 250 ng of siRNA (21 bp, Eurogentec SR-CL010-005) was mixed with lipids at different ratios in 20 μL final volume. 20 μL of each lipoplexes (samples) were mixed with 4 μL of loading buffer (glycerol 30%, (v/v), bromophenol blue 0.25% (w/v), and xylene cyanol 0.25 (w/v)) and subjected to agarose gel electrophoresis for 20 min at 100 V. The electrophoresis gel was visualized and digitally photographed using a G.BOX camera.

Exclusion Assay. Ten microliters of EB (10 mg/mL) was diluted in 580 mL in deionized water. Ten microliters of 90 ng/ μL solution of siRNA was added. A varying amount of lipid (depending on the siRNA/lipid ratio required) was added to the EB solution finally. The solutions were mixed on a benchtop vortex, and the fluorescence was measured (λ_{exc} = 470 nm, λ_{em} = 600 nm; 0.5 cm path length glass cuvette).

ζ Potential and Size Distribution of KNL (with and without siRNA). Experiments were realized with or without siRNA at room temperature. The N/P ratio of 10 (KNL/siRNA) was analysed.

Transmission Electronic Microscopy (TEM). TEM experiments were performed using a Philips CM 10 (negative staining with ammonium molybdate 1% water, Cu/Pd carbon coated grids). Cationic lipoplexes were prepared as described above and were visualized by negative staining microscopy. Ten microliter aliquots of samples (either liposomes or lipoplexes) were transferred to a carbon-coated grid for 10 min. Then, the samples were dried and stained with 2.5% (w/w) of uranyl acetate for 30 s. The specimens were observed with a Hitachi H 7650 electron microscope.

Transfection assays. We have in our lab the HupIRF clone, which stably expresses luciferase. These clones were selected by zeocin antibiotic treatment at 0.5 mg/ml concentration. This stable clone was generated from HuH7, hepatocarcinoma cell line.

The cells are cultured in Dulbecco's Modified Eagle's Medium (D-MEM, Invitrogen) and supplemented with 10% fetal bovine serum (FBS, invitrogen) and Zeocin antibiotic at 0.5 mg/mL at 37 °C in a 5% CO₂ atmosphere. Cells were split every 4–5 days to maintain monolayer coverage. The day before transfection, cells were seeded in 24 well plates (50 000 cells/well). On the day of transfection, the medium containing serum and antibiotic was removed from the well plates and replaced with 200 µL of transfection medium without serum. Lipoplexes were prepared by adding 4 µL of siRNA (20 pmole final amount) in 50 µL of medium without serum and 5 or 10 µL of Ketal vesicles dispersions (0.5 mg/mL). These complexes were left at room temperature for 15 min before being added to the cells. For lipofectamineTM 2000, we followed the protocol provided by the company. The cells were incubated with lipoplexes in a media without serum for 2 or 4 h to permit transient transfection. Afterward, the complex-containing suspension was removed and replaced by 200 µL of the complete growth medium. Transfection efficiency was followed by luciferase assay from Promega.

Luciferase assay and protein quantification:

After 48 hours, the cells were washed by 200 µL of PBS and lysed by adding 100 µL of lysis buffer 1X. After 20 min, 20 µL of cell lysate were added to 100 µL of luciferase substrate and the light intensity was measured. 20 µL of cell lysate were used for protein quantification by Bradford blue. The light intensity was normalized by mg of protein for each condition.

Cell culture

Human prostate cancer (PC-3) cells were purchased from the American Type Culture Collection (Manassas, VA, USA). Cells were maintained in DMEM (Lonza Group Ltd., Switzerland) supplemented with 10% fetal bovine serum (FBS). Cells were maintained at 37°C in a 5% CO₂ humidified atmosphere.

Transfection experiments with PC3 cell line

One day before transfection, 1×10^6 cells were seeded in 10 cm dishes in 10 mL fresh complete medium containing 10% FBS. Before transfection, complexes of siRNA–nucleolipid reagent were prepared.

The desired amount of siRNA (or negative control) and nucleolipid reagent was diluted in 1 mL Opti-MEM transfection medium. The nucleolipid reagent was added to the siRNA solution, homogenized for 10 s with a Vortex, and kept for 20 min at room temperature. Serum-free medium (4 mL) was then added to the complex solution to bring the final volume to 5 mL. Before adding the transfection complexes, the complete medium with serum was removed, and cells were washed once with PBS. The complex solution (5 mL) was then added and incubated at 37°C in the absence or presence of 10% FBS. After incubation for 4 h, the transfection mixture was replaced with complete medium containing 10% FBS, and maintained under normal growth conditions for further incubation for 72 h.

Western blot

Samples containing equal amounts of protein (15 mg) from lysates of cultured PC-3 cells were analyzed by Western blot analysis with 1:5000-diluted rabbit anti-human Hsp27 polyclonal antibody (Stressgen Assay Designs Inc., Michigan, USA) or 1:2500-diluted mouse anti-human vinculin monoclonal antibody (Sigma Chemical Co., St. Louis, MO, USA). Filters were then incubated for 1 h at room temperature with 1:5000-diluted horseradish peroxidase (HRP)-conjugated anti-rabbit or anti-mouse monoclonal antibody (Santa Cruz Biotechnology Inc., Santa Cruz, CA, USA).

Specific proteins were detected using an enhanced chemiluminescence Western blotting analysis system (Amersham Life Science, Arlington Heights, IL, USA).

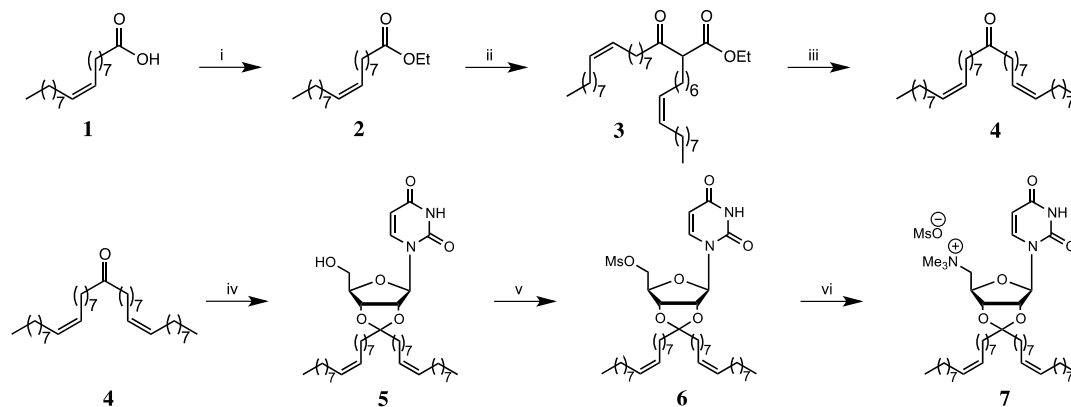
MTT assays

The growth inhibitory effects of Hsp27 siRNA plus nucleolipid on PC-3 cells were assessed by 3-(4,5-dimethylthiazol-2-yl)-2,5-diphenyltetrazolium bromide (MTT) assay (Sigma–Aldrich, Lyon, France).

Briefly, cells were seeded in each well of 24-well microliter plates and allowed to attach overnight. Cells were then treated once daily with nucleolipid for 4 h. MTT assays were carried out after 72 h; each assay was performed in triplicate.

RESULTS AND DISCUSSIONS

Synthesis. In order to evaluate the impact of the lipid structure on the transfection properties, a novel ketal based nucleolipid (KNL) derived from a dihexadec-9-enyl ketal was prepared from oleic acid by a six steps synthetic pathway as shown in Scheme 1. After preparation of the dioleyl ketone **4**, and its coupling reaction with uridine, this intermediate was treated with mesyl chloride to afford the 5'-mesylate nucleoside derivative **6**. This compound was transferred to a pressure tube and treated for 2 days with trimethylamine in THF to give the final ketal derivative **7**.



Reagents and conditions: (i) EtOH, TsOH, toluene, rfx, 12 h, 96%; (ii) EtO⁻Na⁺, EtOH, rfx, 5 h, 49%; (iii) KOH, EtOH, rfx, 4 h, 95%; (iv) Uridine, TsOH, HC(OEt)₃, THF/toluene, rfx, 48 h, 32%; (v) MsCl, DMAP, CH₂Cl₂, rt, 4 h, 75%; (vi) NMe₃, THF, 60°C, 48 h, 74%.

Scheme 1. Synthesis of the dioleyl ketal derivative (KNL: compound 7) starting from oleic acid.

Physicochemical studies.

Transmission Electronic Microscopy, Dynamic Light Scattering.

The morphology of the aggregates obtained with the new ketal nucleolipid in the absence and presence of siRNA was first studied using TEM. First, hydration at room temperature into of the KNL at a concentration of 0.5 mg/mL induces the spontaneous formation of spherical heterodisperse objects of 100 nm in size after extrusion, which are likely liposome-like structures systems (Figure 2A). Under these conditions, at room temperature, the oleyl chains are in a “fluid” state allowing the formation of fluid bilayers. The formation of vesicular systems is consistent with previous reports on phosphocholine uridine derivatives^{xxii} and DOTAU¹⁶.

Transmission electronic microscopy (TEM) experiments performed in the presence of siRNA, with a mixture of KNL and siRNA (ratio = KNL/siRNA: 10) reveal the spontaneous formation of nanoparticles (Figure 2C) with multilamellar organizations similar to lipoplexes (cationic liposome-nucleic acid complexes) with cationic lipids (Figure 2B and 2D, incubation times of siRNA with KNL

for 10 and 1 minutes respectively). As seen on TEM image taken at an early stage, with an incubation time of 1 minute (Figure 2D), the formation of the KNL-siRNA lipoplexes is due to the interactions occurring between KNL based liposomes and siRNA. The resulting self assembly involving both KNL and siRNA molecules leads to well organized nanoparticles where the siRNA is trapped and protected between two KNL bilayers (Figure 2G).

The Zeta potential and size distribution profile of this nucleolipid, alone and in the presence of

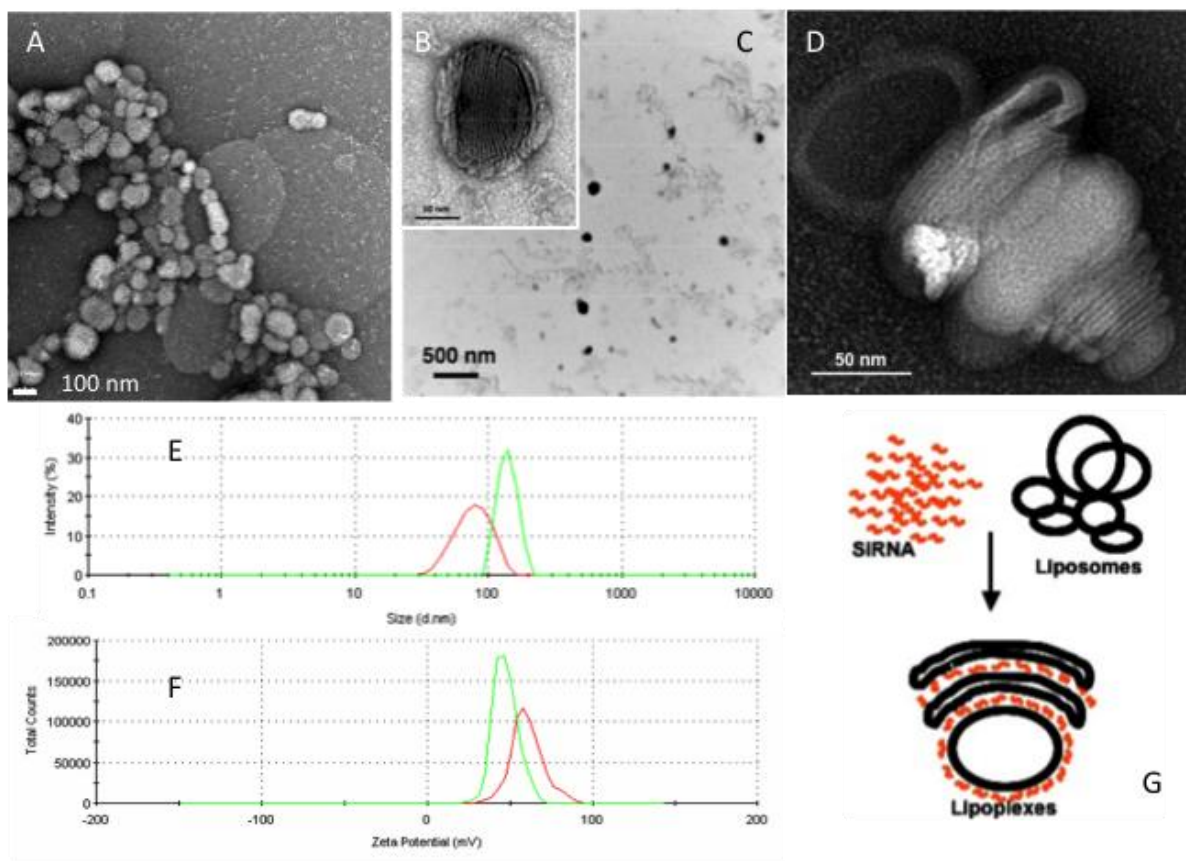


Figure 2. TEM images of KNL in the absence (A) or in the presence of siRNA (B, C and D). B/ magnification of TEM image showing a KNL/siRNA nanoparticle obtained after an incubation time of 10 min. D/ TEM image of multilamellar KNL/siRNA self-assemblies at an early stage (incubation time: 1 min) yielding to nanoparticles loaded with siRNA. E and F/ Size and Zeta potential distributions for aqueous samples obtained in the absence (90 nm, pdi: 0.21 red) and in the presence of siRNA (105 nm, pdi: 0.18 green), respectively. G/ Schematic drawing describing the formation of multilamellar KNL/siRNA self-assemblies.

nucleic acids (N/P ratio : KNL/siRNA= 10), were obtained *via* electrophoretic mobility and Dynamic Light Scattering (DLS) measurements. The results show a decrease of the ζ -potential (Figure 2F), accompanied by an increase of size distribution in the presence of siRNA (Figure 2E), suggesting its complexation with KNL vesicles. The results demonstrate unambiguously that KNL formed nanometer-scale compact spherical complexes entrapping siRNA. These complexes are ~ 100 nm in diameter

(Figure 2C and 2E), a size that is important for efficient endocytosis-mediated cell uptake. The size of the complexes is known to affect delivery efficacy and small particles (up to ~ 150 nm) are typically preferred for *in vivo* applications. Next, we studied the complex formation between KNL and Luciferase siRNA using gel mobility-shift assays and standard ethidium bromide fluorescence displacement assay.

Fluorescence and gel migration studies.

The KNL-siRNA complex formation was confirmed by standard ethidium bromide (EB) fluorescence displacement assay and electrophoresis (Figure 3). The binding affinity of siRNA by KNL was investigated by the fluorescence titration of ethidium bromide (EB). In the presence of siRNA, the fluorescence emission of EB is enhanced relative to that in water as a result of EB intercalation between the RNA base pairs. The subsequent addition of KNL to the siRNA-EB complex solution results in KNL binding to siRNA and displacement of EB from the helix to water, which induces a decrease in fluorescence intensity. With a N/P ratio of KNL/siRNA = 2.6, half of the fluorescence was decreased and all the EB was removed from the siRNA at a N/P ratio of 3.9 (Figure 3). A siRNA (21 bp) gel electrophoresis with a premixed solution of siRNA and various concentrations of KNL was also performed. Results showed that KNL formed complexes with luciferase siRNA and retarded siRNA migration at 5 μ L of the KNL solution (corresponding to a N/P ratio KNL/siRNA = 1.8). Note that stable complexes are observed for higher N/P ratios (see SI, Figure SI 3).

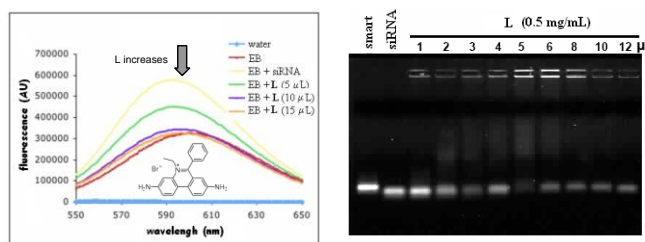


Figure 3. Ethidium bromide (EB) fluorescence displacement assay (Left, KNL/siRNA N/P Ratios: 1.3, 2.6, and 3.9 corresponding to 5, 10 and 15 μ L, respectively). Migration in agarose gel of luciferase siRNA, 1.6 nM/well in the presence of KNL (0.58×10^{-9} mole / μ L). The best complexation is observed for a N/P ratio higher than 1.8 (line 5 μ L of KNL).

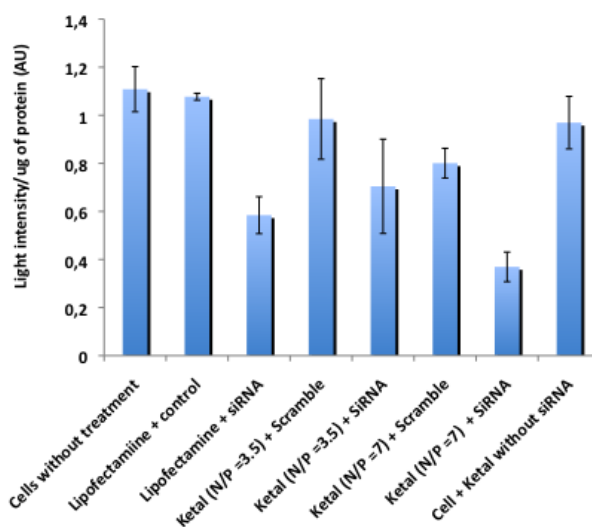


Figure 4. Transfection assays (with KNL/nucleic acid N/P ratios of 3.5, and 7) of stable hepatic cell lines HupIRF, carrying a luciferase reporter gene (incubation time of 2h).

Luciferase down regulation assay siRNA Transfection assays.

Next, we investigated our KNL based nanoparticles loaded with anti-luciferase siRNA, for their transfection properties into stable clone hepatic cell lines HupIRF, carrying a luciferase reporter gene (Figure 4). Increasing the molar ratio of transfecting reagents, including KNL and lipofectamine, results in a decrease of the proteins expression. Note that the KNL 7 was the most effective in siRNA delivery. At a ratio higher than 2, which corresponds to its best complexation ratios as revealed by gel electrophoresis studies (Figures 3 and SI3), lipofectamine show a decrease of 40% of protein production whereas KNL decreases more than 60% of this level of production. Importantly, in similar conditions the diester analogue DOTAU was poorly effective in transfecting siRNA (see Figure SI1). The efficacy KNL for siRNA delivery is due to the presence of the ketal function. We can hypothesize that the formation of stable complexes is attributable to the restricted conformation^{19,20} (ribose C2'-endo corresponding to the south conformation) and/or the increased stability of ketal function (not cleaved by esterase) compared to diester function (DOTAU) in biological conditions.

Transfections of small nucleic acids into human prostate cancer (PC-3) cells using KNL.

Prostate cancer (PC) is one of the most common malignancies in industrialized countries, and the second leading cause of cancer-related deaths. Androgen withdrawal remains the only first line effective form of systemic therapy for men with advanced PC. Unfortunately, castration-resistant (CR) progression occurs within a few years in nearly all cases. Docetaxel is the standard chemotherapy for CRPC; improving median overall survival by ~2-3 months^{xxiii,xxiv}. Recently, two new molecules have been developed and obtained marketing authorisation, cabazitaxel for chemotherapy and the dihydrotestosterone inhibitor called abiraterone improving overall survival for around 8-12 months^{xxv,xxvi,xxvii}. CR progression involves variable combinations of clonal selection, adaptive up-regulation of anti-apoptotic genes, ligand-independent androgen receptor activation and alternative growth factor pathways and immune system escape. Additional therapeutic strategies targeting molecular mechanisms mediating resistance, combined with immunotherapy must be developed. One strategy to improve therapies in advanced PC involves targeting genes that are activated by androgen withdrawal, either to delay or prevent the emergence of the resistant phenotype.

Rocchi *et al.*^{xxviii} have shown that expression of heat shock protein 27 (Hsp27) is up regulated by hormonal ablation and chemotherapy. Hsp27 is an adenosine triphosphate-independent molecular chaperone that is highly induced during stress responses and forms oligomers interacting with a wide variety of proteins, thus preventing their aggregation. Hsp27 is a cell survival protein found at elevated levels in many human cancers including prostate, lung, breast, ovarian, bladder, renal, pancreatic,

multiple myeloma and liver cancers. It has a central role in cellular signalling and is now recognized as an important therapeutic target^{xxxix}. Many anti-cancer therapies are known to further elevate Hsp27 levels. Increased levels of Hsp27 in some human cancers are associated with metastases, poor prognosis and resistance to radiation or chemotherapy. Recently, Hsp27 antisense oligodeoxynucleotides (ASO and second generation OGX-427, a 2'-methoxyethyl modified phosphorothioate oligonucleotide^{xxx}) and short interfering RNA (siRNA) that target the human translation initiation site were reported to potently inhibit Hsp27 expression in human prostate PC-3 cells with concomitant increased caspase-3 cleavage, apoptosis and 87% suppression of cell growth.

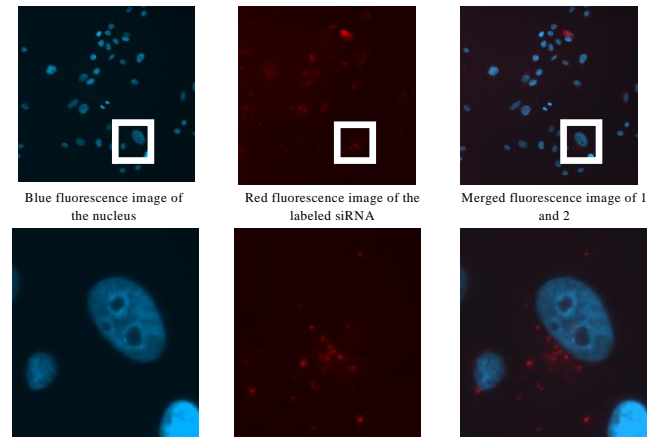


Figure 5: Study of the KNL-mediated uptake of siRNA in PC-3 cells using red fluorescent dye siRNA.

The uptake of the Hsp27 siRNA-KNL complexes by human prostate cancer (PC-3) cells was further investigated by confocal fluorescence imaging. We monitored the KNL-mediated internalization of siRNA in PC-3 cells using red fluorescent dye labeled siRNA. PC-3 cells were treated with red-labeled siRNA-KNL complexes (20 nM siRNA and N/P ratio of 3) for 4 h, and then subjected to staining with blue fluorescent dye DAPI for imaging the nuclei of PC-3 cells. Results presented in figure 5 reveal that red fluorescent siRNA-KNL nanoparticles were located inside PC-3 cells 4 h after treatment with non-silencing siRNA-KNL. These nanometer-scale complexes were found in the cytoplasm, but not in the nuclei of PC-3 cells, as indicated by the distinct red fluorescent nanoparticles and the blue cell nuclei stained by the fluorescent dye DAPI within PC-3 cells as well as the merged image of both. In contrast, after treatment with a similar amount of red siRNA, no red fluorescent signal was observed within the cells.

Next the gene silencing effect resulting from Hsp27 siRNA delivery by KNL in PC-3 cells was assessed. Since the degradation of the targeted mRNA and the corresponding decrease in protein production are the direct consequences of siRNA-mediated gene silencing, the effects of KNL-mediated delivery of Hsp27 siRNA on the levels of protein expression were evaluated. Figure 6 shows the significant knockdown of Hsp27 protein with Hsp27 siRNA-KNL treatment. Hsp27 protein expression levels were determined by western blot analysis using the same protocol as previously described by Rocchi *et al.*^{xxxii} with

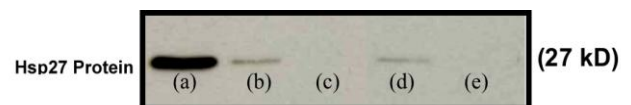


Figure 6: Hsp27 protein levels analyzed by western blotting 3 days post-treatment (a) control (b) oligofectamine + OGX 427 (70 nM) (c) oligofectamine + SiRNA (40 nM) (d) KNL + OGX 427 N/P=3 (e) KNL + SiRNA N/P=3.

vinculin as a reference for protein quantification. The specificity of the observed down-regulation of Hsp27 protein was also demonstrated by a lack of inhibition by KNL alone, Hsp27 siRNA alone, or scramble siRNA-KNL (data not shown). A first series of transfection assays (with different KNL/nucleic acid ratios) of PC-3 cell lines indicated that this new compound is able to transfect the second-generation Hsp27 antisense oligodeoxynucleotides (OGX 427)^{xxxii} and a short interfering RNA (siRNA) and thus to inhibit Hsp27 expression. Note that MTT cytotoxicity assays realized on PC3 cells incubated with KNL at concentrations used for transfection experiments did not revealed any toxicity effect of the KNL (Figure 7D).

Optimal conditions for the delivery of small therapeutic nucleic acids.

The delivery of a small therapeutic nucleic acids (siRNA, antisense) and their associated gene silencing effect depends on their concentrations (Figure 7) and the N/P charge ratio of KNL complexes. Our results revealed a clear siRNA dose-dependent gene silencing. The silencing effect was further

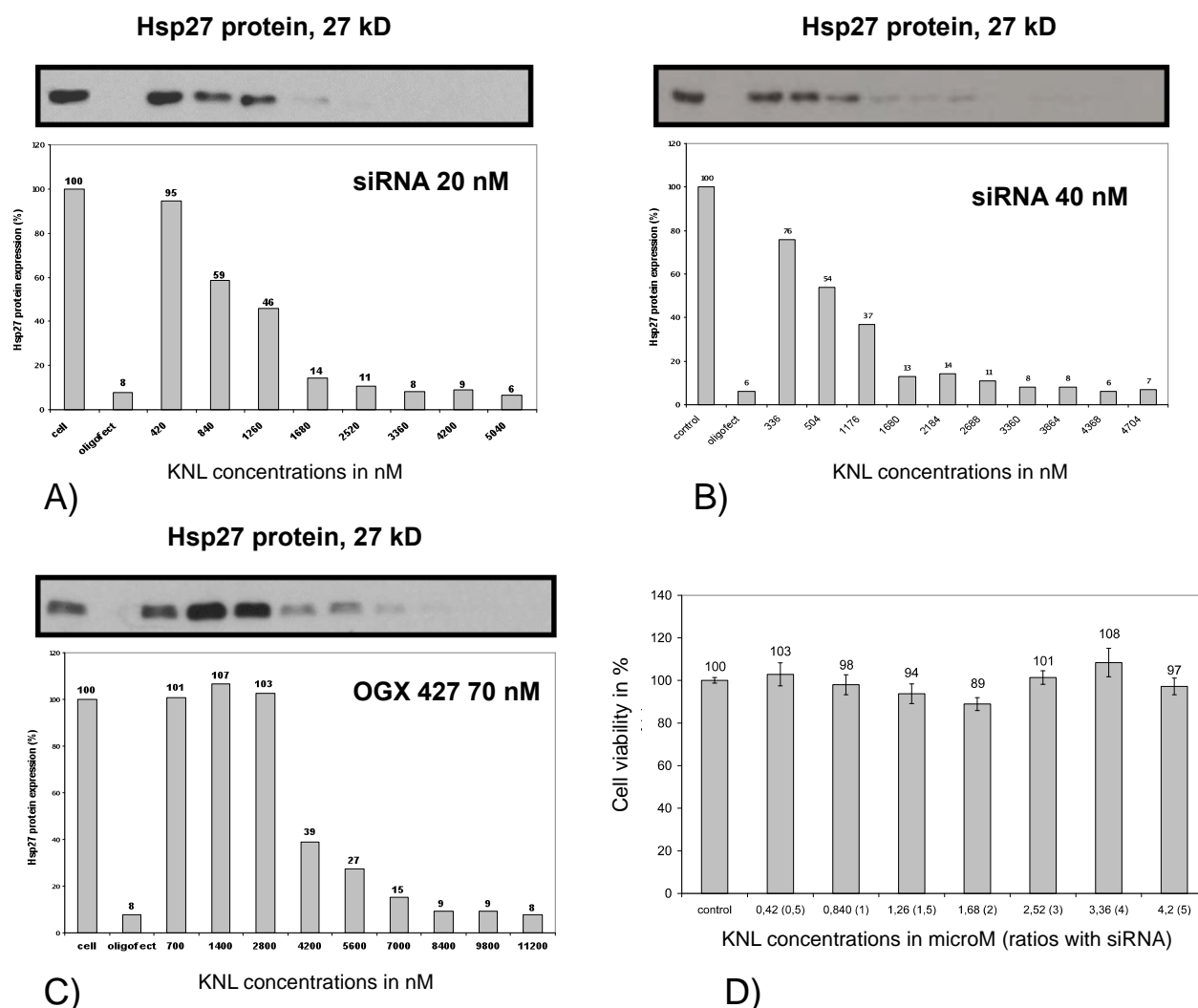


Figure 7: Evaluation of protein expression demonstrates that KNL-mediated Hsp27 siRNA (A and B) or antisense (C) delivery and gene silencing effects depend on N/P ratios. D) Cell viability was assessed using a MTT assay realized on PC3 cells, which were incubated with KNL at different concentrations corresponding to different charge ratios. Oligofectamine is used as positive control in these experiments.

dependent on N/P charge ratio: the higher the N/P number, the more efficient the gene silencing was. An optimal silencing effect was observed with an N/P>2 for siRNA (20 nM) (Figure SI4). By varying the post treatment period and the incubation time, a transfection time of 4 hours and post-treatment of 72 h were identified as optimal conditions for Hsp27 siRNA delivery into PC-3 cells. As shown in Figure 7, treatment of PC-3 cells with KNL/SiRNA or KNL/ASO (OGX427) significantly reduced Hsp27 mRNA levels by up to 85% in a dose-dependent manner, whereas Hsp27 mRNA expression was not significantly suppressed by scrambled oligonucleotide.

CONCLUSION

In summary, we synthesized a new Ketal Nucleotide-based Lipid (KNL) featuring uridine as nucleoside and a dioleoyl ketal as hydrophobic moieties. This new KNL spontaneously self-assembles to form liposome-like structures in aqueous solutions as revealed by DLS and Electronic Microscopy studies. Electrophoresis experiments and standard ethidium bromide fluorescence displacement assay indicate that KNL binds luciferase siRNA at an optimal ratio of 7. This observation was confirmed by TEM experiments, which show the spontaneous formation of nanoparticles of roughly 100 nm in diameter. The study of transfection ability of KNL realized on stable hepatic cell lines HupIRF demonstrate that KNL is able to transfect siRNA and exhibits protein knockdown more efficiently than its diester analogue (DOTAU) and lipofectamineTM 2000. In line with previous studies for cationic lipids,^{14,15} the ketal function inserted into the nucleolipid structure facilitates the delivery of siRNA and gene silencing activity. Considering the high transfection efficiency observed of the KNL nanoparticles for luciferase siRNA, we evaluated the ability of KNL to transfect therapeutic small nucleic acids including siRNA and antisense oligonucleotides. Importantly, in this work we demonstrate that KNL transfects siRNA and antisense (OGX-427) efficiently and completely inhibits Hsp27 expression in human prostate PC-3 cells. Such an inhibition has been reported to induce the suppression of cancer cell growth. Taken together, the present findings demonstrate that a minor small structural variation (ketal linker) in nucleoside lipids molecular structure can profoundly influence small nucleic acid-binding characteristics and consequently gene delivery efficacies of the corresponding nanoparticles. Novel therapeutic approaches involving either siRNA or antisense oligonucleotide might take advantage of the KNL characteristics.

ACKNOWLEDGMENT

This work has been supported by the French National Agency (ANR) in the frame of its programmes EmergenceBio and Blanc: i) project NANOVA, n°ANR-08-EBIO-013-01 and project GelCells, appel à projets Blanc SIMI 7-2010, respectively. We acknowledge the Army Research Office and INSERM for financial support.

REFERENCES

- [i] Jin, J., Bae, K. H., Yang, H., Lee, S. J., Kim, H., Kim, Y., Joo, K. M., Seo, S. W., Park, T. G., and Nam, D. H. *In Vivo* Specific Delivery of c-Met siRNA to Glioblastoma Using Cationic Solid Lipid Nanoparticles. *Bioconjugate Chem.* (2011), 22, 2568–2572.
- [ii] Sioud, M., and Mobergslien, A. Efficient siRNA Targeted Delivery into Cancer Cells by Gastrin-Releasing Peptides. *Bioconjugate Chem.* (2012), 23, 1040–1049.
- [iii] Dorn, G., Patel, S., Wotherspoon, G., Hemmings-Mieszczak, M., Barclay, J., Natt, F. J., Martin, P., Bevan, S., Fox, A., Ganju, P., Wishart, W., and Hall, J. siRNA relieves chronic neuropathic pain. *Nucleic Acids Res.* (2004), 32, e49.
- [iv] Novina, C. D. and Sharp P. A. The RNAi revolution. *Nature.* (2004), 430, 161-164.
- [v] Raouane, M., Desmaële, D., Urbinati, G., Massaad-Massade, L., and Couvreur, P. Lipid Conjugated Oligonucleotides: A Useful Strategy for Delivery. *Bioconjugate Chem.* (2012), 23, 1091–1104.
- [vi] Merkel, O. M., Zheng, M., Debus, H., and Kissel, T. Pulmonary Gene Delivery Using Polymeric Nonviral Vectors. *Bioconjugate Chem.* (2012), 23, 3–20.
- [vii] Troiber, C., and Wagner, E., Nucleic Acid Carriers Based on Precise Polymer Conjugates. *Bioconjugate Chem.* (2011), 22, 1737–1752.
- [viii] Tseng, Y. C., Mozumdar, S., and Huang, L. *Advanced Drug Delivery Reviews* (2009), 61, 721–731.
- [ix] Kaiden, T., Yuba, E., Harada, A., Sakanishi, Y., and Kono, K. Dual Signal-Responsive Liposomes for Temperature-Controlled Cytoplasmic Delivery. *Bioconjugate Chem.* (2011), 22, 1909–1915.

- [x] Asayama, S., Kumagai, T., and Kawakami H. Synthesis and Characterization of Methylated Poly(L-histidine) To Control the Stability of Its siRNA Polyion Complexes for RNAi. *Bioconjugate Chem.* (2012), 23, 1437–1442.
- [xi] Takemoto, H., Miyata, K., Ishii, T., Hattori, S., Osawa, S., Nishiyama, N., and Kataoka K. Accelerated Polymer–Polymer Click Conjugation by Freeze–Thaw Treatment. *Bioconjugate Chem.* (2012), 23, 1503–1506.
- [xii] Jin, H., Lovell J. F, Chen J., Lin Q., Ding L., Ng K. K., Pandey R. K., Manoharan M., Zhang Z., and Zheng G. Mechanistic insights into LDL nanoparticle-mediated siRNA delivery. *Bioconjugate Chem.* (2012), 23, 33–41.
- [xiii] Juliano, R. L., Ming, X., and Nakagawa, O. Cellular Uptake and Intracellular Trafficking of Antisense and siRNA Oligonucleotides. *Bioconjugate Chem.* (2012), 23, 147–157.
- [xiv] Semple, S. C., Akinc, A., Chen, J., Sandhu, A. P., Mui, B. L., Cho, C. K., Sah, D. W. Y., Stebbing, D., Crosley, E. J., Yaworski, E., Hafez, I. M., Dorkin, J. R., Qin, J., Lam, K., Rajeev, K. G., Wong, K. F., Jeffs, L. B., Nechev, L., Eisenhardt, M. L., Jayaraman, M., Kazem, M., Maier, M. A., Srinivasulu, M., Weinstein, M. J., Chen, Q., Alvarez, R., Barros, S. A., De, S., Klimuk, S. K., Borland, T., Kosovrast, V., Cantley, W. L., Tam, Y.K., Manoharan, M., Ciufolini, M. A., Tracy, M. A., de Fougères, A., MacLachlan, I., Cullis, P. R., Madden, T. D., and Hope, M. J. Rational design of cationic lipids for siRNA delivery. *Nature Biotechnology* (2010), 28, 172–176.
- [xv] Sato, Y., Hatakeyama, H., Sakurai, Y., Hyod, M., Akita, H., and Harashima, H. A pH-sensitive cationic lipid facilitates the delivery of liposomal siRNA and gene silencing activity in vitro and in vivo. *J. Control. Release* (2012), 163, 267–276.
- [xvi] Chabaud, P., Camplo, M., Payet, D., Serin, G., Moreau, L., Barthélémy, P., and Grinstaff, M. W. Cationic nucleoside lipids derived for gene delivery. *Bioconjugate Chem.* (2006), 17, 466–472.
- [xvii] Ceballos, C., Prata, C. H., Giorgio, S., Payet, D., Barthélémy, P., Grinstaff, M. W., and Camplo, M. Cationic nucleoside lipids possessing a 3-nitropyrrole universal base for siRNA delivery. *Bioconjugate Chem.* (2009), 20, 193–196.

- [xviii] Ceballos, C., Khiati, S., Prata, C. A., Zhang, X. X., Giorgio, S., Marsal, P., Grinstaff, M. W., Barthélémy, P., and Camplo, M. Cationic Nucleoside Lipids Derived from Universal Bases: A Rational Approach for siRNA Transfection, *Bioconjugate Chem.* (2010), 21, 1062-1069.
- [xix] Taib, N., Aimé, A., Moreau, L., Camplo, M., Houmadi, S., Desbat, B., Laguerre, M., Grinstaff, M.W., Bestel, I. and Barthélémy, P. Formation of supramolecular systems via directed Nucleoside-Lipid recognition. *J. Colloid Interface Sci.* (2012), 377, 122-130.
- [xx] Moreau, L., Camplo, M., Wathier, M., Taib, N., Laguerre, M., Bestel, I., Grinstaff, M. W., and Barthélémy, P. Real time imaging of supramolecular assembly formation via programmed nucleolipid recognition. *J. Am. Chem. Soc.* (2008), 130, 14454-14455.
- [xxi] Pinnarat, T., and Savage, P.E. Non catalytic esterification of oleic acid in ethanol. *Journal of Supercritical Fluids* (2010), 53, 53-59.
- [xxii] Moreau, L., Barthélémy, P., El Maataoui, M., Grinstaff, M. W. Supramolecular assemblies of nucleoside phosphocholine amphiphiles. *J. Am. Chem. Soc.* (2004), 126, 7533-7539.
- [xxiii] Petrylak, D. P., Tangen, C. M., Hussain, M. H., Lara, P. N. Jr, Jones, J. A., Taplin, M. E., Burch, P. A., Berry, D., Moinpour, C., Kohli, M., Benson, M. C., Small, E. J., Raghavan, D., and Crawford, E. D. Docetaxel and estramustine compared with mitoxantrone and prednisone for advanced refractory prostate cancer. *N. Engl. J. Med.* (2004), 351, 1513-1520.
- [xxiv] Tannock, I. F., de Wit, R., Berry, W. R., Horti, J., Pluzanska, A., Chi, K. N., Oudard, S., Théodore, C., James, N. D., Turesson, I., Rosenthal, M. A., and Eisenberger, M. A., Docetaxel plus prednisone or mitoxantrone plus prednisone for advanced prostate cancer. *N. Engl. J. Med.* 351, (2004), 1502-1512.
- [xxv] Matos, C. S., de Carvalho, A. L., Lopes, R. P., and Marques, M. P. New strategies against prostate cancer-Pt(II)-based chemotherapy. *Curr. Med. Chem.* (2012), 19, 4678-87.
- [xxvi] Malhotra, M., Dhingra, R., Sharma, T., Deep, A., Narasimhan, B., Phogat, P., and Sharma P. C. Cabazitaxel: A Novel Drug for Hormone-Refractory Prostate Cancer. *Mini Rev. Med. Chem.* (2012), 12, 1-6.

- [xxvii] Miyake, H., Pollak, M. and Gleave, M. Castration-induced up-regulation of insulin-like growth factor binding protein-5 potentiates insulin-like growth factor-I activity and accelerates progression to androgen independence in prostate cancer models. *Cancer Res.* (2000), 60, 3058-3064.
- [xxviii] Andrieu, C., Taieb, D., Baylot, V., Ettinger, S., Soubeyran, P., De-Thonel, A., Nelson, C., Garrido, C., So, A., Fazli, L., Bladou, F., Gleave, M., Iovanna, J. L., and Rocchi, P. Heat Shock protein 27 confers resistance to androgen ablation and chemotherapy in prostate cancer cells through , eIF4E. *Oncogene* (2010) 29, 1883.
- [xxix] Acunzo, J., Katsogiannou, M., and Rocchi, P. Small heat shock proteins HSP27 (HspB1), α B-crystallin (HspB5) and HSP22 (HspB8) as regulators of cell death. *Int. J. Biochem. Cell Biol.* (2012), 44, 1622-1631.
- [xxx] Gleave, M. E., and Monia, B. P. Antisense therapy for cancer. *Nature Reviews Cancer* (2005), 5, 468.
- [xxxii] Rocchi, P., So, A., Kojima, S., Signaevsky, M., Beraldi, E., Fazli, L., Hurtado-Coll, A., Yamanaka, K., and Gleave, M. Heat shock protein 27 increases after androgen ablation and plays a cytoprotective role in hormone-refractory prostate cancer. *Cancer Res.* (2004), 64, 6595-6602.
- [xxxii] Kamada, M., So, A., Muramaki, M., Rocchi, P., Beraldi, E., and Gleave, M. Hsp27 knockdown using nucleotide-based therapies inhibit tumor growth and enhance chemotherapy in human bladder cancer cells. *Mol. Cancer Ther.* (2007), 6, 299-308.